

# **Data processing and interpretation of momentum-dependent Electron Energy-Loss Spectroscopy spectra**

Jeroen Sangers

22nd June 2021





# **Data processing and interpretation of momentum-dependent Electron Energy-Loss Spectroscopy spectra**

Jeroen Sangers  
4645197

Supervisor:  
Dr. S. Conesa-Boj  
TU Delft, Faculty of Applied Sciences

Student:  
Sangers, Jeroen  
TU Delft, BSc program Applied Physics

## **Abstract**

placeholder

# Contents

<b>Abstract</b>	<b>ii</b>
<b>Table of contents</b>	<b>iii</b>
<b>1 Introduction</b>	<b>1</b>
<b>2 Theory</b>	<b>2</b>
2.1 The Transmission electron microscope . . . . .	2
2.2 Crystal structure . . . . .	3
2.3 Electron scattering theory . . . . .	3
2.4 Momentum resolved electron energy-loss spectroscopy . . . . .	4
2.4.1 Energy filtered transmission electron microscope . . . . .	5
2.5 Physical relevance of (MR)EELS data . . . . .	5
2.6 q-EELS spectra and q-EELS map . . . . .	5
<b>3 Experimental Method</b>	<b>7</b>
3.1 Data format . . . . .	7
3.2 Data correction techniques . . . . .	8
3.2.1 Removing/altering values . . . . .	8
3.2.2 Zero-loss peak and Batson correction . . . . .	8
3.3 Data processing techniques . . . . .	8
3.3.1 Integration techniques . . . . .	8
3.3.2 Slicing techniques . . . . .	9
3.4 Data extraction . . . . .	9
<b>4 Results</b>	<b>10</b>
4.1 Comparing integration techniques . . . . .	10
4.2 Comparing Batson correction . . . . .	10
4.3 Interesting features from data . . . . .	10
<b>5 Discussion</b>	<b>13</b>
<b>6 Conclusion</b>	<b>14</b>
<b>List of references</b>	<b>15</b>
<b>Appendix</b>	<b>16</b>

# **1 Introduction**

...

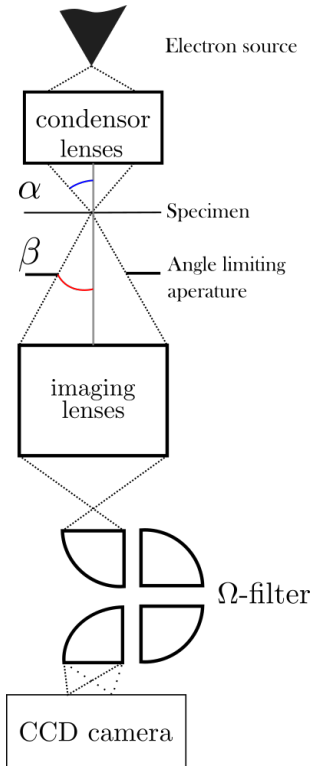


Figure 1: TEM

## 2 Theory

### 2.1 The Transmission electron microscope

The Transmission electron microscope (TEM) is a microscope that far exceeds the capabilities of a normal light microscope. Both types of microscope use a series of lenses to magnify the image of a specimen. A normal light microscope can amplify an image up to about  $1500\times$  and is limited by the diffraction limit. Assuming an average wavelength of  $550\text{nm}$  for green light a high-end microscope is limited to resolving features  $100\text{nm}$  apart. This limit is too low for looking at atomic structures. [1]

An electron microscope circumvents this limit by using electrons, not light, to probe the specimen. Electrons when accelerated have a smaller wavelength than light thus allowing for images with resolved features as small as  $0.05\text{nm}$ . [2] The TEM works by releasing electrons from an electron source and accelerating them to an energy typically expressed in kilo-electronvolt. After being accelerated the electrons pass multiple electromagnetic lenses and a condenser aperture to shape the beam before it 'illuminates' the specimen as illustrated in 1. The beam incident on the sample is limited to a illumination semi-angle  $\alpha$  which is inversely proportional to the resolution, but limiting  $\alpha$  decreases the amount of electrons incident on the specimen and thus a frame needs more time for a decent exposure. After having interacted with the specimen the beam is again limited by an aperture, this aperture sets the collection semi-angle  $\beta$  which controls the limit of scattering angles allowed into the imaging lenses. After the beam is conditioned by the imaging lenses it passes through four electromagnetic prisms which make up an energy filter called an  $\Omega$ -filter named after the shape it needs to have to keep the TEM stack aligned with the CCD-camera to limit aberrations. The  $\Omega$ -filter is used for energy filtered TEM images discussed in section 2.4.1.

Two types of images can be made with the TEM, a normal image which shows the magnified sample and a diffraction pattern image which can be made by placing the capture device in the focal point of the lens and filter system. A diffraction mode image shows the diffraction peaks that are characteristic of the sample and yields information on the reciprocal lattice of the sample. [3]

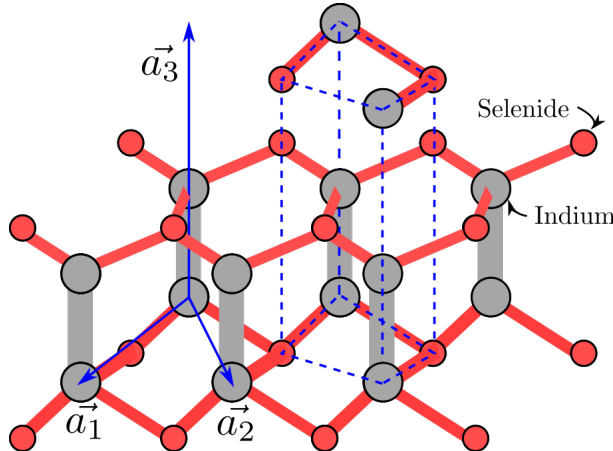


Figure 2: insee

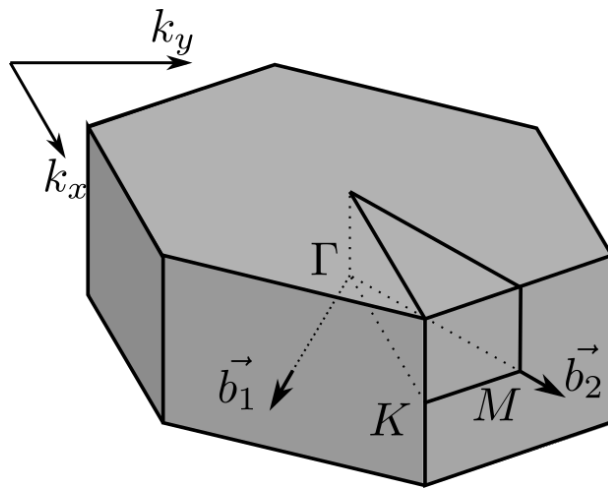


Figure 3: unit

## 2.2 Crystal structure

A crystal is build up of unit cells in such a way that the whole crystal can be made by shifting and aligning unit cells. These unit cells are build up of atoms whose position in the unit cell can be fully expressed in terms of primitive basis vectors. If the crystal were to be cut in half by a plane this plane would be expressed by fractional coordinates, these fractional coordinates show where along a basis vector the plane and basis vector intersect. Such a plane is called a Miller plane and the corresponding coordinates are called the Miller indices. Miller planes that have the same orientation but are shifted to different unit cells share the same Miller indices and are called a family of planes. The crystal structure of  $\gamma$ -IndiumSelenide with its basis vectors and unit cell is shown in figure 2. In reciprocal space the diffraction spots correspond to a certain family of planes, the position of diffraction spots can be expressed in reciprocal basis vectors. A reciprocal basis unit cell is shown in figure 3. In this figure the high-symmetry directions are also shown as arrows.

## 2.3 Electron scattering theory

In a TEM setup electrons are essentially shot through a sample in which the electrons can either simply pass through or scatter, in the latter scenario there are two possibilities, electrons can scatter elastically or inelastically. Scattering is a result of the interaction between the sampling electrons from the TEM source and the charges particles in the specimen.

When scattering elastically the electrons interact with a nucleus of the specimen whose mass is many times greater than that of the sampling electron, resulting in a small and usually unmeasurable energy transfer.

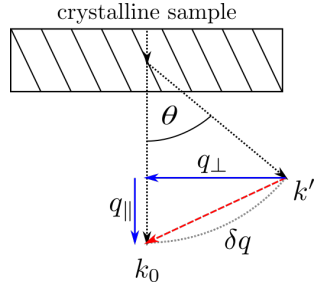


Figure 4: The elastic scattering  $k'$  of an electron over an angle  $\theta$  due to the interaction with a crystalline sample.

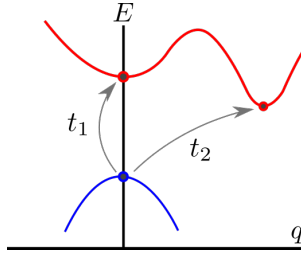


Figure 5: The band structure of the crystalline sample in fig. 4 showing both a direct bandgap  $t_1$  and an indirect bandgap  $t_2$ .

In a crystalline specimen electrons can only be scattered at certain angles due to the crystal structure creating a diffraction pattern of bright spots. In cases of large scattering angles the electron does transfer a significant amount of energy and can even reverse direction, this energy transfer can permanently displace atoms in the crystal structure causing a defect.

When the sampling electron interacts with an electron in the specimen's crystal lattice inelastic occurs due to the similarity in mass between the two electrons. The energy transfer of this interaction ranges from a few electronvolts up to multiple hundreds of electronvolts. Inelastic scattering not only results in an energy transfer but also in a momentum transfer as shown in figure 4, the  $k'$ -vector shows a scattered electron that deviates from the not scattered electron vector  $k_0$ . The total momentum transfer is the sum of the perpendicular momentum transfer  $q_{\perp}$  proportional to the scattering angle  $\theta$  and the momentum transfer parallel to the undisturbed path due to an energy transfer from the sampling electron to the sample. This parallel momentum transfer is thus proportional to the energy loss of the electron. Figure 5 shows the band structure of the crystalline sample of which the electrons scatter. In this figure two bands are shown, both bands can be occupied by electrons of certain energies, to excite an electron from the blue band to the red band an electron needs either energy (path  $t_1$ ) or energy and momentum (path  $t_2$ ). The needed energy and momentum are transferred from an incident sampling electron in the inelastic interaction. By measuring the energy and momentum of a scattered electron it is possible to piece together all the combinations of energy and momenta transfer possible and thus find the band structure of the sample.

Another form of inelastic scattering is plasmon excitation.

Since the outer-shell electrons of an atom are only weakly bound to the nucleus due to screening effects but are coupled together by electrostatic interaction. These delocalised electrons form an energy band similar to that shown in figure 5. When a fast-moving sampling electron is shot through the sample all nearby outer-shell electrons are displaced. If the sampling electron's velocity exceeds the fermi speed the displacement of outer-shell electrons creates an oscillating ripple creating waves of alternating positive and negative electric charge, this is known as a plasmon wake.

## 2.4 Momentum resolved electron energy-loss spectroscopy

Momentum resolved electron energy-loss spectroscopy hereafter abbreviated as MREELS is a TEM imaging technique in which the imaging plane of the CCD camera is placed in the focal point of the imaging lenses and energy filter. This allows the camera to take a diffraction mode image in which the diffraction pattern of the scattering electrons is shown. This is illustrated in figure 6. In this figure the crystalline sample

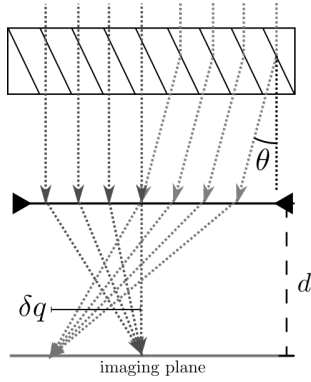


Figure 6: scat

is shown as the box with the slanted lines that represent the Miller planes of the crystal structure. As shown in the figure all electrons that scatter off of the same family of Miller planes get focused on the same region on the imaging sensor, electrons that do not scatter also get focused in one spot at the centre of the diffraction pattern. A diffraction mode image does not image normal space but instead shows reciprocal space which is also the reason this type of image is useful. In a normal image one would attribute lengths to the axes of an image but in a diffraction mode image the separation of features is given by a momentum difference. The separation of the light and dark grey arrows on the imaging plane in figure 6 is thus equal to the difference in perpendicular momentum transfer between scattering electrons (light grey) and electrons that do not scatter (dark grey). Since the momentum transfer for the electrons that do not scatter is zero the momentum transfer for scattering of a certain family of planes can be determined.

#### 2.4.1 Energy filtered transmission electron microscope

An energy filtered transmission electron microscope is a microscope with an energy filter placed in the optical column of the TEM. Energy filtering is accomplished by the use of electromagnetic prisms such as those shown in figure 8. These prisms just like ordinary prism disperse the electrons with different wavelengths proportional to electron energy. By sliding a slit into the cone of dispersed electrons it is possible to choose a finite range of electron energies to image. The EFTEM setup can be used in conjunction with the MREELS imaging technique to gather information on both the momentum transfer of the electron (via MREELS) and the energy loss associated (via EFTEM) with that momentum transfer.

### 2.5 Physical relevance of (MR)EELS data

As hinted at in section 2.4, the combination of both energy and momentum information allows for the reconstruction of the band structure of the specimen. This information can be used to determine the density of states of the specimen [4] [3]. EELS spectra can also be used to determine the electronic properties of the specimen, the bandgap of a semiconductor and the dielectric function, as well as mechanical properties [3]. Different signature peaks in the EELS data can be used to determine the elemental makeup of the specimen [3].

### 2.6 q-EELS spectra and q-EELS map

+zlp

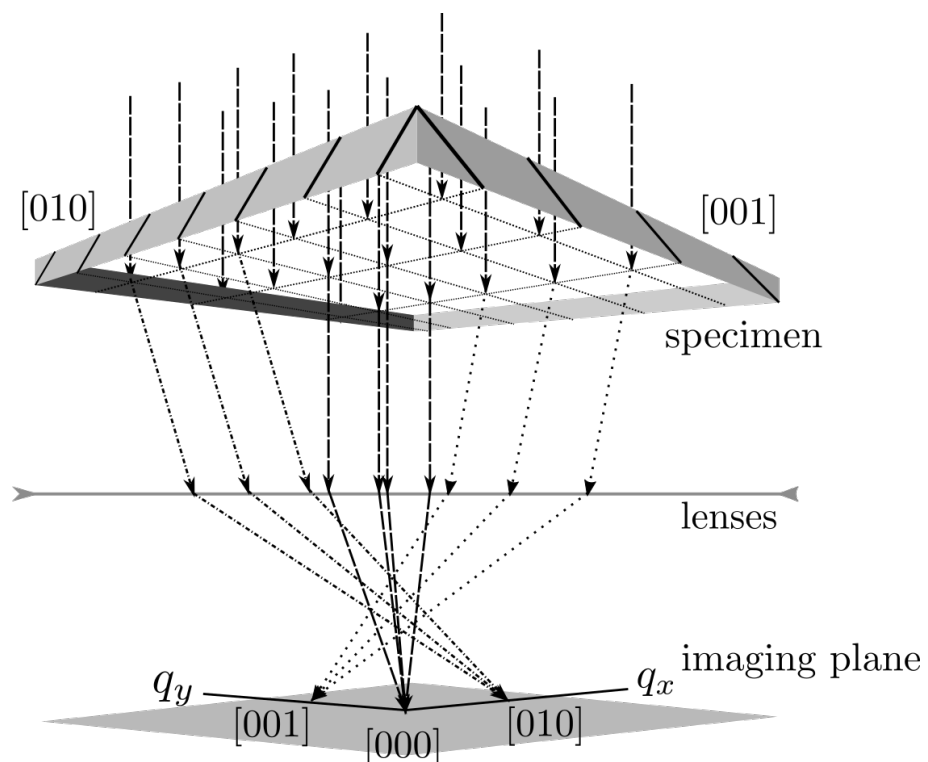


Figure 7: scat

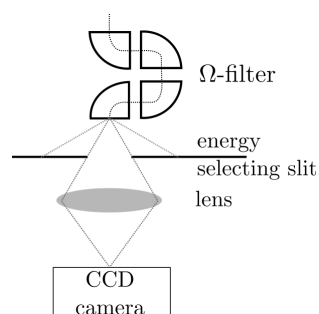


Figure 8: A  $\Omega$ -spectrometer spreading the electrons based on their energy and a slit selecting energies to focus on the CCD camera.

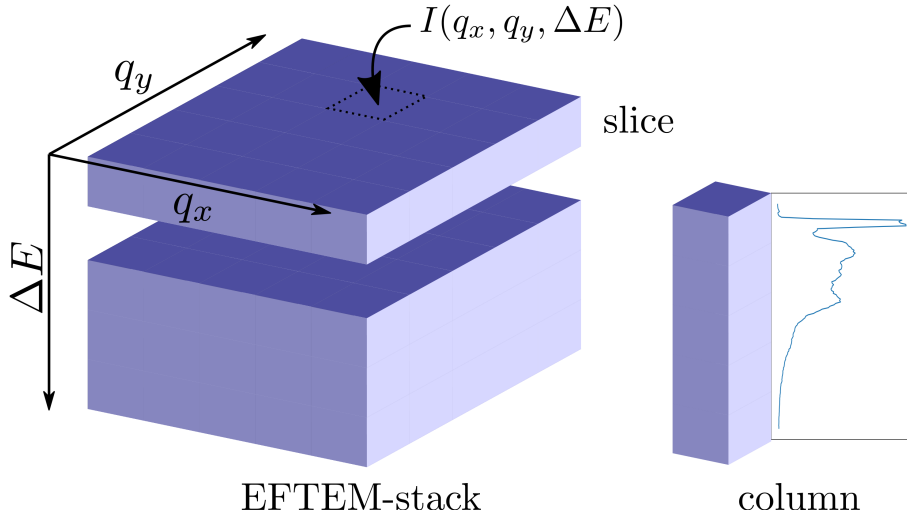


Figure 9: An illustration of an EFTEM-stack, slice, column and corresponding axes.

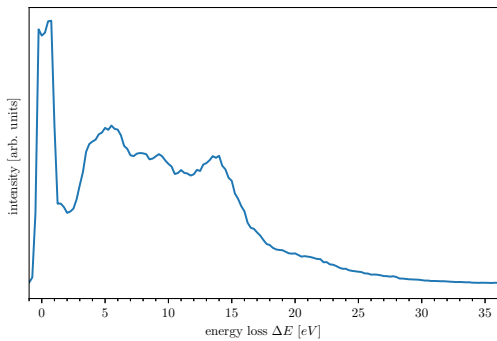


Figure 10: EELS spectrum of  $\gamma$ -InSe for  $q_{\perp} = 0$

### 3 Experimental Method

#### 3.1 Data format

For this work a specimen of  $\gamma$ -InSe was imaged using the momentum resolved electron energy loss technique in an energy filtered transmission electron microscope. The file was supplied with aligned zero-loss peaks in Gatan's .dm4 format which had to be converted to a python object for further data processing in python, for the conversion from Gatan's proprietary file to a python object the excellent ncempy package [5] was used.

The measurement data is gathered by taking energy filtered diffraction images at different energy losses. All these images are stacked corresponding to their energy loss value, resulting in a EFTEM image stack as illustrated in figure 9. In the illustrated cube the horizontal planes or slices are diffraction mode images associated with an energy loss  $\Delta E$ , these energy slices have their own momentum axes that are not necessarily aligned with the whole stack. After alignment the individual pixels in the EFTEM stack can be fully expressed by four values, three coordinates:  $q_x$ ,  $q_y$ ,  $\Delta E$  and one scattering intensity  $I$ .

An example of such a spectrum is illustrated in figure 10. Another way is to extract multiple of these columns such that their total momentum increases, doing this yields a energy-momentum map as pictured in figure 11. Once the EFTEM stack is aligned it is possible to start extracting sets of values in meaningful ways. One way is to take a single column from the top of the stack to the bottom, doing this results in a 1D-array of values for a set position in momentum space and varying energy-loss, this is called an electron energy loss spectrum.

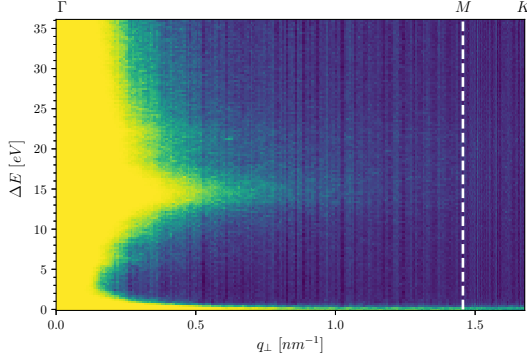


Figure 11: q-EELS map of  $\gamma$ -InSe along  $\Gamma \rightarrow M \rightarrow K$

## 3.2 Data correction techniques

### 3.2.1 Removing/altering values

Before any meaningful results can be extracted from the EFTEM stack it is important to first correct the data. This process starts by removing all the values corresponding to negative energy losses, these values are can be incorrectly indexed as a result of the microscope software aligning the slices such that the zero-loss peak is at an energy loss of 0eV. It does this by shifting slices up or down to match them to their true energy loss, slices corresponding to negative energy losses are duplicates of slices at positive energy losses.

After removing the negative energy loss slices the negative intensity values are raised by the minimum amount needed to make all values positive. This means that all values of the entire stack are raised by the absolute value of the most negative intensity. Doing this changes the performance of further techniques for the better.

Since the acquisition time of the EFTEM stack is quite large and not all slices are taken at the same time it might happen that the sample moves due to disturbances. Correcting this is done by convoluting a slice with Sobel matrices to get an edge-detected image, these images are then aligned by means of Fourier phase correlation [6].

### 3.2.2 Zero-loss peak and Batson correction

To try and remove the zero-loss peak of the q-EELS spectrum a Batson correction is performed. A Batson correction normally uses the sum of all EELS spectra in an EFTEM image of the sample to try and correct plural scattering and subtract the zero-loss peak [7]. Since such an image was not available the sum of all q-EELS spectra in the first Brillouin zone was used since this region was more likely to correspond to a true image of the sample, the sum of the q-EELS spectra in the first Brillouin zone is called the correction spectrum. The Batson correction is then performed by scaling the correction spectrum for each q-EELS spectra to be corrected in such a way that the integrated intensity of the zero-loss peaks matches, then the "centre of intensity" of the zero-loss peaks is determined and the correction spectrum is subtracted from the to be corrected q-EELS spectra with the centres of intensity aligned.

## 3.3 Data processing techniques

Since the EFTEM data is essentially a 3D cube of values it needs to be processed in such a way that the information it contains can be extracted. This is something that can not be done with the cube itself since it is hard to represent 3D data in meaningful ways.

### 3.3.1 Integration techniques

To achieve the goal of representing the data in a meaningful ways two integration techniques have been implemented in Python. A radial integration method that finds the centre of the image stack which is determined to be the brightest pixel of the unaltered EFTEM stack since this is most probably the zero-loss peak at the centre of the unscattered beam. From this centre outward the method sums all EELS

spectra in circle from a certain radius to that radius plus a ringsize, the starting and ending radius as well as the ringsize can be specified by the user. This method is the same as integrating with respect to the solid angle but without the appropriate constants involved. When this method is finished the result is an array of summed EELS spectra for a set of rings. This can be plotted as a momentum-energy EELS map as shown in 11. Instead of integration in circle segments over the entire stack the user might want to only do a line-like integration towards a single diffraction peak. If this is the case a similar method to the one described above is called except for the change that instead of circle segments it integrates over pie piece like segments.

### 3.3.2 Slicing techniques

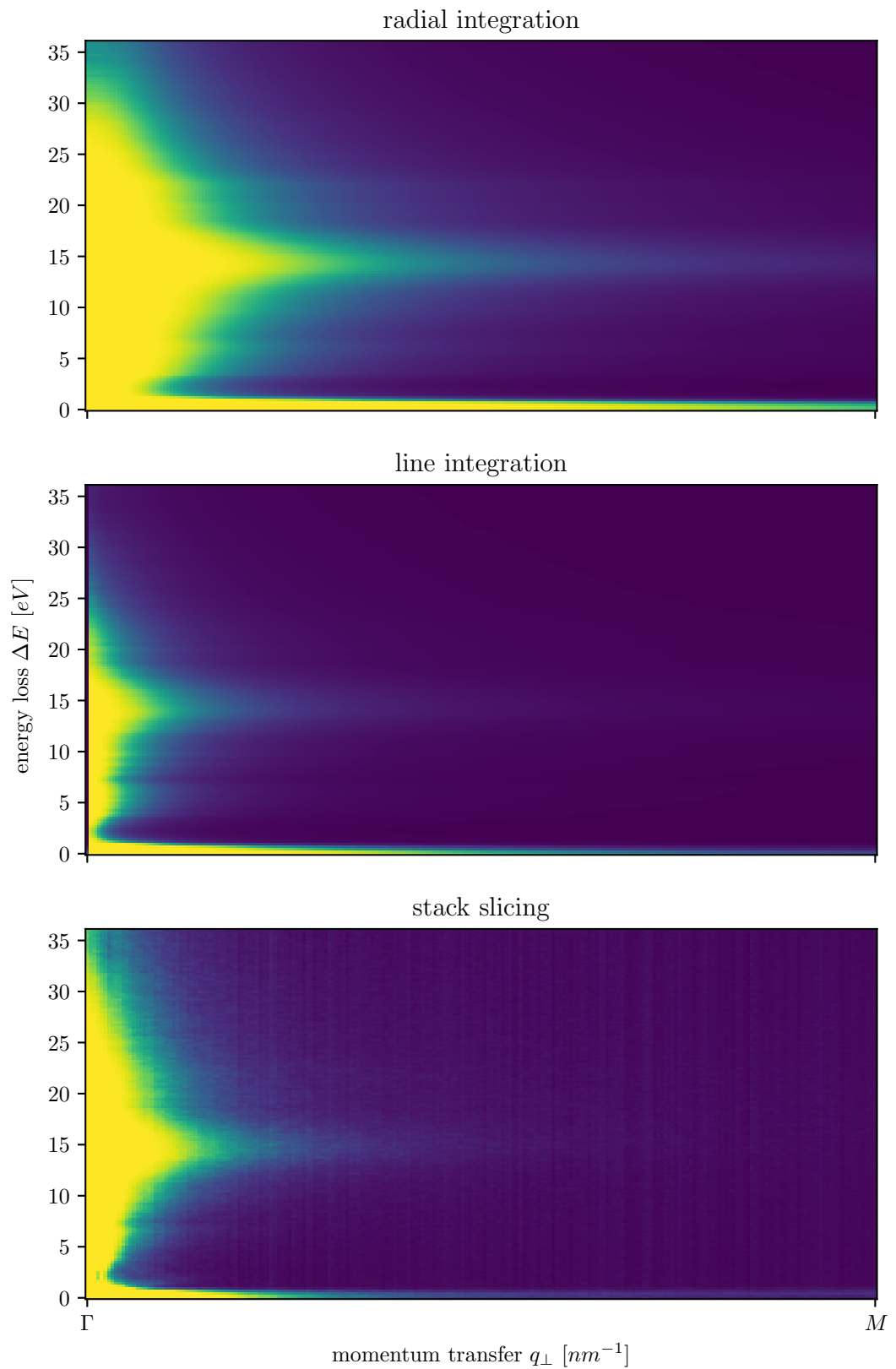
Slicing refers to the term of "array slicing" in Python/Numpy which is the built-in way to select data from an array whose position in the array satisfies a condition. The slicing technique allows the user to specify one or two points and extracts all columns along the line between the two points. If one point is specified by the user the other point will be the centre of the EFTEM stack. This method returns an array of all the EELS spectra for the points along the line. This can again be plotted as a momentum-energy map.

## 3.4 Data extraction

Once the full 3D EFTEM stack is reduced to useful momentum-energy maps or  $q$ -EELS spectra it is possible to start identifying interesting features such as peaks in the  $q$ -EELS spectra at certain regions or bright spots in the momentum-energy maps. For instance, if long bright streaks can be observed in the momentum-energy map they might hint at a relation between energy and momentum of an often occurring reaction. One of such bright peaks that will be tracked is the plasmon peak at roughly  $14.5eV$  energy loss.

## **4 Results**

- 4.1 Comparing integration techniques**
- 4.2 Comparing Batson correction**
- 4.3 Interesting features from data**



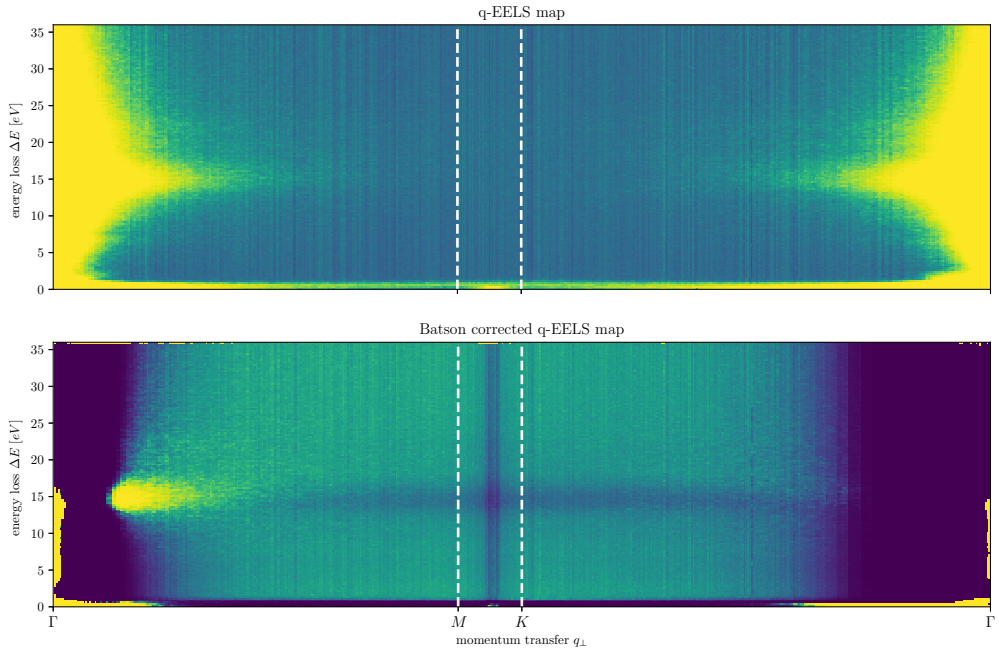


Figure 13: Batson correction for qmap

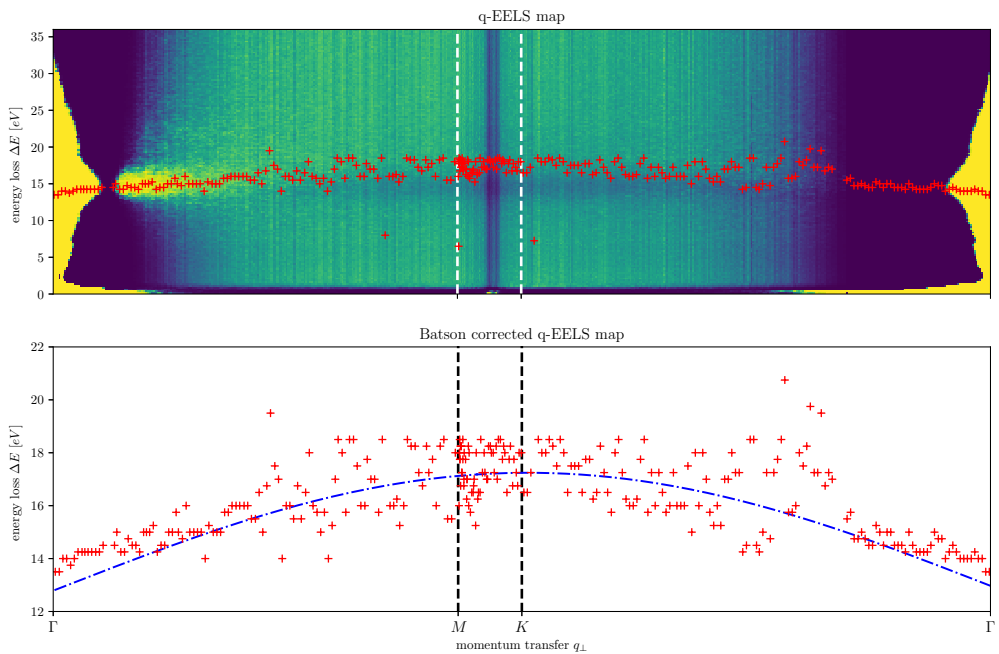


Figure 14: tracked peaks on stitched qmap

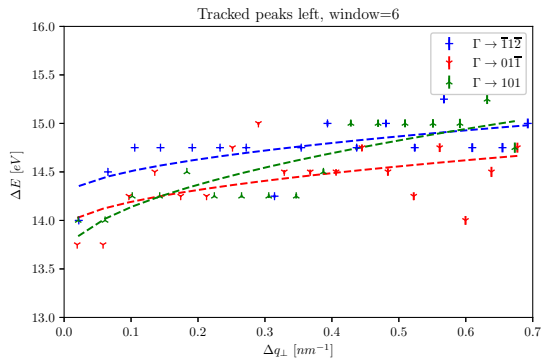


Figure 15: Tracked peaks of the plasmon dispersion.

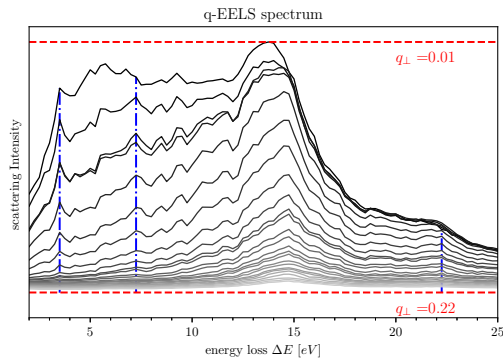


Figure 16: Tracked peaks of the plasmon dispersion.

## 5 Discussion

...

## 6 Conclusion

placeholder

## References

- [1] E. G. van Putten, D. Akbulut, J. Bertolotti, W. L. Vos, A. Lagendijk, and A. P. Mosk, “Scattering lens resolves sub-100 nm structures with visible light,” *Phys. Rev. Lett.*, vol. 106, p. 193905, May 2011.
- [2] C. Kisielowski, B. Freitag, M. Bischoff, H. van Lin, S. Lazar, G. Knippels, P. Tiemeijer, M. van der Stam, S. von Harrach, M. Stekelenburg, and et al., “Detection of single atoms and buried defects in three dimensions by aberration-corrected electron microscope with 0.5-Å information limit,” *Microscopy and Microanalysis*, vol. 14, no. 5, p. 469477, 2008.
- [3] R. F. Egerton, “Electron energy-loss spectroscopy in the TEM,” *Reports on Progress in Physics*, vol. 72, p. 016502, dec 2008.
- [4] E. Gaufrès, F. Fossard, V. Gosselin, L. Sponza, F. Ducastelle, Z. Li, S. G. Louie, R. Martel, M. Côté, and A. Loiseau, “Momentum-resolved dielectric response of free-standing mono-, bi-, and trilayer black phosphorus,” *Nano Letters*, vol. 19, no. 11, pp. 8303–8310, 2019. PMID: 31603690.
- [5] P. Ercius, P. Gonzalo, T. Schoonjans, fniekiel, tcpekin, and koschie, “ncempy.” The last three authors are github usernames.
- [6] M. Sjödahl and L. R. Benckert, “Electronic speckle photography: analysis of an algorithm giving the displacement with subpixel accuracy,” *Appl. Opt.*, vol. 32, pp. 2278–2284, May 1993.
- [7] P. E. Batson and J. Silcox, “Experimental energy-loss function,  $\text{Im}[-\frac{1}{\epsilon}(q, \omega)]$ , for aluminum,” *Phys. Rev. B*, vol. 27, pp. 5224–5239, May 1983.

# Appendix

Placeholder and code block test

## Python

The python code used to calculate the ellipse axes is displayed below.

```
1 def ellipse_calc(x,y):
2     # replace nans by average
3     x_ = np.where(np.isnan(x), np.nanmean(x), x)
4     y_ = np.where(np.isnan(y), np.nanmean(y), y)
5
6     # Calculate variance and covariance
7     var_x = np.sum((x_-np.mean(x_))**2)/(len(x)+1)
8     var_y = np.sum((y_-np.mean(y_))**2)/(len(y)+1)
9     cov = np.sum((x_-np.mean(x_))*(y_-np.mean(y_))/(len(x_)+1))
10
11    cov_matrix = np.asarray([[var_x, cov],[cov, var_y]])
12    evals, evecs = linalg.eig(cov_matrix)
13    evecs_ = evals*evecs
14    #plt.plot(x,y, linestyle='none', marker='x', zorder=1)
15    #plt.quiver(np.nanmean(x),np.nanmean(y),-evecs_[1,:],-evecs_[0,:],
16    zorder=2, units='xy', scale=1, width=1e-8, headwidth=4)
17
18    a = np.max(evals)
19    b = np.min(evals)
20    print(a)
21    print(b)
22    index_a = np.where(evals == a)[0]
23    theta = np.arctan(evecs[0,index_a]/evecs[1,index_a])
24    print('theta =', theta)
25    return a,b,theta
26
```